

Commun. Theor. Phys. **75** (2023) 105102 (9pp) https://doi.org/10.1088/1572-9494/acf304

Nonlinear and non-CP gates for Bloch vector amplification

Michael R Geller

Center for Simulational Physics, University of Georgia, Athens, GA 30602, United States of America

E-mail: mgeller@uga.edu

Received 6 July 2023, revised 12 August 2023
Accepted for publication 23 August 2023
Published 21 September 2023

Abstract

Any state $\boldsymbol{r} = (x, y, z)$ of a qubit, written in the Pauli basis and initialized in the pure state $\boldsymbol{r} = (0, 0, 1)$, can be prepared by composing three quantum operations: two unitary rotation gates to reach a pure state $\boldsymbol{r} = (x^2 + y^2 + z^2)^{-\frac{1}{2}} \times (x, y, z)$ on the Bloch sphere, followed by a depolarization gate to decrease $|\boldsymbol{r}|$. Here we discuss the complementary state-preparation protocol for qubits initialized at the center of the Bloch ball, $\boldsymbol{r} = \boldsymbol{0}$, based on increasing or amplifying $|\boldsymbol{r}|$ to its desired value, then rotating. Bloch vector amplification increases purity and decreases entropy. Amplification can be achieved with a linear Markovian completely positive trace-preserving (CPTP) channel by placing the channel's fixed point away from $\boldsymbol{r} = \boldsymbol{0}$, making it nonunital, but the resulting gate suffers from a critical slowing down as that fixed point is approached. Here we consider alternative designs based on linear and nonlinear Markovian PTP channels, which offer benefits relative to linear CPTP channels, namely fast Bloch vector amplification without deceleration. These gates simulate a reversal of the thermodynamic arrow of time for the qubit and would provide striking experimental demonstrations of non-CP dynamics.

Keywords: nonlinear channels, non-completely positive channels, Bloch vector amplification

(Some figures may appear in colour only in the online journal)

Several papers have explored the use of real or effective quantum nonlinearity for information processing [1–17]. Nonlinear master equations have also been frequently discussed in open systems theory [18–32]. In this paper we go beyond the paradigm of linear CPTP maps to design single-qubit gates that increase the length of the Bloch vector without changing its direction. It is well known that this operation can be implemented using linear Markovian completely positive trace-preserving (CPTP) channels, via the Gorini–Kossakowski–Sudarshan–Lindblad (GKSL) master equation [33, 34]. This provides a baseline which we call the linear CPTP amplification gate. The nonunital channel behind it is entropy decreasing, which is possible in an open system that compensates by producing enough environmental entropy as to not violate the second law. In addition to the linear CPTP gate, we also consider alternatives based on non-completely positive (non-CP) and nonlinear channels. The channels considered here are Markovian normalized PTP channels taking the form $X \mapsto \phi(X)/\mathrm{tr}[\phi(X)]$, where $\phi(X)$ is a continuous 1-parameter positive linear or nonlinear map satisfying $\mathrm{tr}[\phi(X)] \neq 0$ for all positive semidefinite (PSD) operators X. Normalized PTP channels fall into 4 classes, yielding 3 distinct forms of nonlinearity [35]:

(i) *Linear PTP*: linear ϕ and $\mathrm{tr}[\phi(X)] = 1$ for all X;
(ii) *NINO*: linear ϕ and $\mathrm{tr}[\phi(X)] \neq 1$ for some X;

(iii) *State-dependent PTP*: nonlinear ϕ and $\mathrm{tr}[\phi(X)] = 1$ for all X;

(iv) *General normalized PTP*: nonlinear ϕ and $\mathrm{tr}[\phi(X)] \neq 1$ for some X.

The linear CPTP gate belongs to class (i). A non-CP gate from class (i) will also be considered. Class (ii) leads to a restricted form of nonlinearity, where a diagonal nonlinear term is added to the master equation to conserve trace. This type of evolution equation extends a pure-state nonlinear Schrödinger equation first introduced by Gisin [18] in 1981, to mixed states [23, 24, 26, 30, 35]. Rembieliński and Caban [36] recently argued that this type of nonlinearity is causal

(does not support superluminal signaling) and should not be excluded from a fundamental theory. We call these channels nonlinear in normalization only (NINO) to emphasize their restricted form of nonlinearity. In section 2, several amplification gates based on NINO channels are investigated. Class (iii) channels include unitary mean field theories such as the Gross–Pitaevskii equation for weakly interacting bosons, and they support Bloch-ball torsion, believed to be a powerful computational resource [1–3, 8, 14, 35]. Our main result is a non-CP gate from class (i) and we do not discuss channels from class (iii) or (iv) in this paper.

Quantum channels that are positive but not completely positive, or non-CP, are well known in open systems theory [25, 37–40], and are used to detect entanglement [41]. However the question of whether non-CP channels could provide a *computational* advantage over linear CPTP channels appears to be largely unexplored [25], although they have been shown to increase channel capacity [42–44] in communication settings. Here we find an advantage for Bloch vector amplification, also called repolarization [25], and propose that an experimental demonstration of 'fast' amplification would constitute a striking demonstration of a physical non-CP map.

1. PSD cone

For the analysis of linear qubit channels it is sufficient to take, as the state space of a qubit, the Bloch sphere or ball, and to study the dynamics within that space. Here we will work in the larger space of PSD operators $X \succcurlyeq 0$ with strictly positive trace $\tau := \mathrm{tr}(X)$, a convex but noncompact set called the PSD cone.[1] Allowing density matrices to have a trace differing from the canonical value $\tau = 1$ is a straightforward extension of pure state quantum mechanics with square-integrable but unnormalized wave functions, and is equivalent to the canonical formulation as long as expectation values $\langle A\rangle := \mathrm{tr}(XA)/\mathrm{tr}(X)$ are properly defined, and $\mathrm{tr}(X) \neq 0$. There is little benefit to using the PSD cone representation with linear PTP channels due to their property of conserving τ for any initial value (this condition is part of their definition). However nonlinear PTP channels allow for a more restricted implementation of trace preservation, where the trace is conserved only if the initial trace has the canonical value $\tau = 1$. The PSD cone representation elucidates the mechanism of trace conservation in these cases. Let X: $\mathcal{H} \to \mathcal{H}$ be a linear operator on the system Hilbert space $\mathcal{H} = (\mathrm{span}\{|e_i\rangle\}_{i=1}^N, \langle x|y\rangle)$, with complete orthonormal basis $\{|e_i\rangle\}_{i=1}^N$ and inner product $\langle x|y\rangle = \sum_{i=1}^N x_i^* y_i$, and let $X^\dagger$ denote the adjoint of X with respect to $\langle x|y\rangle$. x^* denotes complex conjugation and I_N is the $N \times N$ identity. The set of bounded linear operators form a complex vector space $B(\mathcal{H}, \mathbb{C})$. Let $\mathrm{Her}(\mathcal{H}, \mathbb{C}) = \{X \in B(\mathcal{H}, \mathbb{C}): X = X^\dagger\}$ and $\mathrm{Her}^{\geqslant 0}(\mathcal{H}, \mathbb{C}) = \{X \in \mathrm{Her}(\mathcal{H}): X \succcurlyeq 0\}$ be the subsets of self-adjoint and PSD operators, respectively. In the qubit case, $N = 2$, any $X \in \mathrm{Her}(\mathcal{H}, \mathbb{C})$ can be written in the Pauli basis as

$$X = \frac{\tau I_2 + r^a \sigma^a}{2} = \frac{1}{2}\begin{pmatrix} \tau + z & x - iy \\ x + iy & \tau - z \end{pmatrix},$$
$$\mathrm{spec}(X) = \frac{\tau \pm \sqrt{x^2 + y^2 + z^2}}{2}. \quad (1)$$

Here $\tau, r^a \in \mathbb{R}$, $a \in \{1, 2, 3\}$, and $\mathrm{spec}(X)$ contains the eigenvalues. The conditions for X to be in $\mathrm{Her}^{\geqslant 0}(\mathcal{H}, \mathbb{C})$ are (i) $\tau \geqslant 0$ and (ii) $|\boldsymbol{r}| = \sqrt{x^2 + y^2 + z^2} \leqslant \tau$. For each $\tau > 0$, the vector $\boldsymbol{r} = (x, y, z)$ must lie within a ball of radius τ centered at $\boldsymbol{r} = 0$, defining a cone in $\mathbb{R}^4$ oriented along τ. A 3D representation of this state space is given in figure 1.

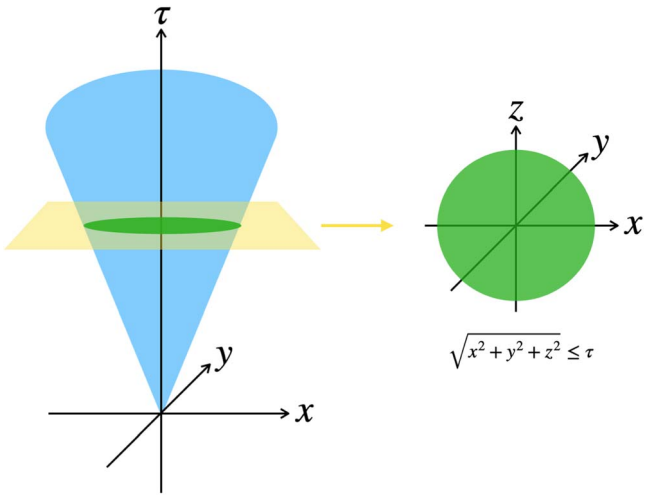

Figure 1. Extended state space of a qubit. On the left, the subspace with fixed trace is shown as a green circle, but it is really a Bloch ball with radius τ.

The physical interpretation of the Bloch vector is slightly different in the PSD cone picture. Namely, $r^a = \mathrm{tr}(\sigma^a X)$ is equal to the expectation $\langle\sigma^a\rangle = \mathrm{tr}(\sigma^a X)/\mathrm{tr}(X)$ of Pauli matrix σ^a times τ:

$$r^a = \mathrm{tr}(\sigma^a X) = \langle\sigma^a\rangle \tau. \quad (2)$$

The condition defining pure states is also modified. Let $\rho = X/\tau = \rho^2$ be a canonically normalized pure state. Therefore X is pure if and only if

$$X^2 = \mathrm{tr}(X)\, X = \tau\, X. \quad (3)$$

Using (1) we see that these pure states lie on the surface of the PSD cone $|\boldsymbol{r}| = \tau$, as expected.

2. Linear and NINO channels

In this paper we examine Bloch vector amplification gates based on the following NINO model [23, 24, 26, 30, 35]:

$$\frac{\mathrm{d}X}{\mathrm{d}t} = \{L_+, X\} + \sum_\alpha \zeta_\alpha B_\alpha X B_\alpha^\dagger + g\ \mathrm{tr}(X\Omega)X,$$
$$\frac{\mathrm{d}\tau}{\mathrm{d}t} = (g\tau - 1)\ \mathrm{tr}(X\Omega),\ \ \tau = \mathrm{tr}(X), \quad (4)$$

[1] The PSD condition $X \succcurlyeq 0$ implies $\mathrm{tr}(X) \geqslant 0$. We further require that $\mathrm{tr}(X) \neq 0$, excluding the state $X = 0$ at the apex of the cone.

Table 1. Jump operators used in this paper. The σ^1, σ^2, σ^3 are Pauli matrices. The $m \in \mathbb{R}$ are constants determining mean jump frequencies, which we assume to be individually controllable.

α	B_α	$B_\alpha^\dagger B_\alpha$	$B_\alpha B_\alpha^\dagger$	ξ_α	G_α	C_α
0	$m(\sigma^2 + i\sigma^3)$	$2m^2(I_2 - \sigma^1)$	$2m^2(I_2 + \sigma^1)$	$m(0, 0, 1, i)$	$m^2\begin{pmatrix}-2&0&0\\0&0&0\\0&0&0\end{pmatrix}$	$m^2\begin{pmatrix}2\\0\\0\end{pmatrix}$
1	$m(\sigma^1 + \sigma^2)$	$2m^2 I_2$	$2m^2 I_2$	$m(0, 1, 1, 0)$	$m^2\begin{pmatrix}0&2&0\\2&0&0\\0&0&-2\end{pmatrix}$	0
2	$m(I_2 + \sigma^3)$	$2m^2(I_2 + \sigma^3)$	$2m^2(I_2 + \sigma^3)$	$m(1, 0, 0, 1)$	$m^2\begin{pmatrix}0&0&0\\0&0&0\\0&0&2\end{pmatrix}$	$m^2\begin{pmatrix}0\\0\\2\end{pmatrix}$
3	$m\sigma^3$	$m^2 I_2$	$m^2 I_2$	$m(0, 0, 0, 1)$	$m^2\begin{pmatrix}-1&0&0\\0&-1&0\\0&0&1\end{pmatrix}$	0

$$\Omega \coloneqq -2L_+ - \sum_\alpha \zeta_\alpha B_\alpha^\dagger B_\alpha. \tag{5}$$

Here $X \succcurlyeq 0$ represents a (possibly unnormalized) qubit state. Time evolution consists of a smooth part plus random discontinuous jumps. The linear infinitesimal generator L of the smooth part has been decomposed into Hermitian and anti-Hermitian components: $L_\pm = (L \pm L^\dagger)/2$. Equivalently, we can say that $H = \mathrm{i}L$ is the qubit Hamiltonian, which is non-Hermitian when $L_+ \neq 0$. We expand the dissipative part L_+ in the Pauli basis as

$$L_+ = \ell_\mu \sigma^\mu, \quad \sigma^\mu = (I_2, \sigma^1, \sigma^2, \sigma^3), \quad \ell_\mu \in \mathbb{R}^4. \tag{6}$$

The anti-Hermitian part L_- generates unitary evolution. Because amplification is purely nonunitary, we set L_- to zero. The $B_\alpha \in B(\mathcal{H}, \mathbb{C})$ are a set of linearly independent jump operators. The $\zeta_\alpha = \pm 1$ are signs of the Choi matrix eigenvalues (all nonnegative for CPTP channels). Any jump operator with $\zeta_\alpha = -1$ indicates a non-CP channel [37–40]. $g \in \mathbb{R}$ controls the strength of the nonlinear term. The observable $\Omega \in \mathrm{Her}(\mathcal{H}, \mathbb{C})$ is chosen to conserve trace and plays an important role in NINO channels because it governs the dynamics in the τ direction of the PSD cone.

The trace equation in (4) shows that there are two distinct ways to achieve trace-conservation $\mathrm{d}\tau/\mathrm{d}t = 0$: The first is the linear option, $g = 0$, which requires $\Omega = 0$ and leads to the GKSL equation and the linear CPTP gate (if the ζ_α are positive). The linear option conserves trace for any initial τ. The second option is to make use of the nonlinearity and fix $g = 1$, leading to the NINO gates. In this case

$$\frac{\mathrm{d}\tau}{\mathrm{d}t} = (\tau - 1)\,\mathrm{tr}(X\Omega). \tag{7}$$

This conserves trace if τ starts with the canonical value $\tau = 1$. The $\tau = 1$ plane in the PSD cone is a fixed plane of the channel. The fixed plane is locally stable wherever $\mathrm{tr}(X\Omega) \leqslant 0$. The operator Ω can lead to an intricate fixed point structure in the PSD cone, including instabilities in dynamically *inaccessible* regions of the cone that nevertheless leave their imprint on the accessible regions in an intuitive way.

The NINO model (4) has a continuous symmetry that is absent (pushed to infinity) in the linear model: Under

$$L_+ \mapsto L_+ + cI_2, \; c \in R \tag{8}$$

we have

$$\Omega \mapsto \Omega - 2cI_2 \tag{9}$$

and

$$\frac{\mathrm{d}X}{\mathrm{d}t} \mapsto \frac{\mathrm{d}X}{\mathrm{d}t} + 2c(1 - g\tau)X, \tag{10}$$

so the equation of motion is invariant if

$$g\tau = 1. \tag{11}$$

The condition (11) is the same as that for trace conservation in (4). Note that the jump operators do not change under this transformation. In certain cases this symmetry can be used to map a NINO channel to a dual linear channel (section 2.4).

We will consider a sequence of increasingly complex NINO channels and amplification gates constructed from a set of jump operators $\{B_0, B_1, B_2, B_3\}$ listed in table 1, combined with specific values of L_+. By amplification we mean a process that smoothly increases $|\boldsymbol{r}|$ from 0 to τ. Without loss of generality we can amplify along the x axis of the Bloch ball. The first jump operator B_0 in table 1 is chosen to produce x-axis amplification in the linear CPTP limit (when combined with an appropriate L_+). The additional jump operators allow for increased control over the fixed points of the map. The amplification gates assume that the qubit is initially prepared in the state $X = \frac{I_2}{2}$, so they require a nonunital channel or an unstable fixed point. Note that

$$\left(\frac{\mathrm{d}X}{\mathrm{d}t}\right)_{\frac{I_2}{2}} = L_+ + \frac{1}{2}\sum_\alpha \zeta_\alpha B_\alpha B_\alpha^\dagger + g\frac{\mathrm{tr}(\Omega)}{4}$$
$$I_2 = \frac{1}{2}\sum_\alpha \zeta_\alpha [B_\alpha, B_\alpha^\dagger] - \frac{\Omega}{2} + g\frac{\mathrm{tr}(\Omega)}{4} I_2. \tag{12}$$

In the linear theory, $g = \Omega = 0$, this expression recovers the well known result that a nonunital Markovian channel requires one or more nonnormal jump operators. However in a NINO channel with $\Omega \neq 0$ we can implement nonunital maps with normal jump operators or even with no jump operators (section 2.2).

In the Pauli basis (4) becomes

$$\frac{\mathrm{d}r^a}{\mathrm{d}t} = \mathrm{tr}\left(\sigma^a \frac{\mathrm{d}X}{\mathrm{d}t}\right) = G^{ab}_{L_+} r^b + C^a_{L_+}\tau + \sum_\alpha \zeta_\alpha (G^{ab}_\alpha r^b + C^a_\alpha \tau) + g\ \mathrm{tr}(X\Omega)\, r^a. \tag{13}$$

The first and second terms on the right side of (13) come from the $\{L_+,\ X\}$ term in (4). Here $G_{L_+} = \mathrm{tr}(L_+)I_3$ and $C^a_{L_+} = \mathrm{tr}(\sigma^a L_+) = 2\ell_a$. The summation over α in (13) contains the contributions

$$G^{ab}_\alpha = \mathrm{tr}(\sigma^a B_\alpha \sigma^b B^\dagger_\alpha)/2 \ \text{ and } \ C^a_\alpha = \mathrm{tr}(\sigma^a B_\alpha B^\dagger_\alpha)/2 \tag{14}$$

from one or more jump operators. Expanding any $B \in \mathbb{C}^{2\times 2}$ in complex coordinates

$$B = \xi_\mu \sigma^\mu,\ \ \sigma^\mu = (I_2, \sigma^1, \sigma^2, \sigma^3),\ \ \xi_\mu \in \mathbb{C}^4 \tag{15}$$

leads to $G^{ab}_\alpha = (|\xi_0|^2 - |\xi_1|^2 - |\xi_2|^2 - |\xi_3|^2)\ \delta^{ab} + 2\,\mathrm{Im}\,(\xi^*_0\xi_c)\varepsilon^{abc} + 2\,\mathrm{Re}(\xi^*_a\xi_b)$. The resulting G_α matrices for each jump operator are given in table 1. The last term in (13) containing $\mathrm{tr}(X\Omega) = (\tau\ \mathrm{tr}(\Omega) + \boldsymbol{r}\cdot\mathrm{tr}(\boldsymbol{\sigma}\Omega))/2$ is diagonal and nonlinear. The vectors C_{L_+}, $C_\alpha \in \mathbb{R}^3$ determine the initial velocity $\mathrm{d}X/\mathrm{d}t$, nonunitality, and fixed points of the channel. These are also given in table 1.

2.1. Linear CPTP

If $g = 0$, the trace equation in (4) requires that $\Omega = 0$, leading to the linear channel

$$\frac{\mathrm{d}X}{\mathrm{d}t} = \{L_+, X\} + \sum_\alpha \zeta_\alpha B_\alpha X B^\dagger_\alpha,\quad \frac{\mathrm{d}\tau}{\mathrm{d}t} = 0,\ \ L_+ = -\frac{1}{2}\sum_\alpha \zeta_\alpha B^\dagger_\alpha B_\alpha. \tag{16}$$

If the $\zeta_\alpha = 1$ then (16) reduces to the GKSL master equation and the map is CPTP. Here we will consider a model with a single jump operator B_0 from table 1 with $\zeta_0 = 1$:

$$\frac{\mathrm{d}X}{\mathrm{d}t} = \{L_+, X\} + B_0 X B^\dagger_0,\ \ \frac{d\tau}{\mathrm{d}t} = 0,\quad L_+ = -\frac{B^\dagger_0 B_0}{2} = m^2(\sigma^1 - I_2). \tag{17}$$

The requirement $\Omega = 0$ imposes conditions $\ell_0 = -m^2$, $\ell_1 = m^2$, $\ell_2 = 0$, and $\ell_3 = 0$ on L_+. In the Pauli basis

$$\frac{\mathrm{d}r^a}{\mathrm{d}t} = G^{ab}r^b + C^a\tau,\quad G = G_{L_+} + G_0 = m^2\begin{pmatrix}-4 & 0 & 0\\ 0 & -2 & 0\\ 0 & 0 & -2\end{pmatrix},\quad C = C_{L_+} + C_0 = m^2\begin{pmatrix}4\\0\\0\end{pmatrix}, \tag{18}$$

leading to the equations of motion

$$\frac{\mathrm{d}x}{\mathrm{d}t} = 4m^2(\tau - x), \tag{19}$$

$$\frac{\mathrm{d}y}{\mathrm{d}t} = -2m^2 y, \tag{20}$$

$$\frac{\mathrm{d}z}{\mathrm{d}t} = -2m^2 z. \tag{21}$$

The solution giving the desired Bloch vector amplification gate is

$$x(t) = (1 - \mathrm{e}^{-4m^2 t})\tau,\ \ x(0) = 0,\quad x(\infty) = \tau,\ \ y, z = 0. \tag{22}$$

The channel has a single stable fixed point at $\boldsymbol{r}^{\mathrm{fp}} = (\tau, 0, 0)$, but the velocity decreases as this fixed point is approached. Due to this critical slowing down, it takes infinitely long to reach the pure state at $x = \tau$, although it becomes exponentially close for $t \gg 1/4m^2$. To quantify the critical slowing down, let $\delta = \tau - x \geqslant 0$. Thus dx/dt vanishes linearly with δ at the fixed point $\delta = 0$.

2.2. No-jump NINO

The first NINO gates we consider are variations on the linear CPTP gate. The simplest is an amplification gate is based on (4) with $g = 1$ and no jump operators. The single model parameter is L_+, which we take to be $L_+ = \ell_0 I_2 + \ell_1\sigma^1$, $\ell_0,\ \ell_1 \in \mathbb{R}$, as in (17). The equation of motion for the no-jump NINO model is

$$\frac{\mathrm{d}X}{\mathrm{d}t} = \{L_+, X\} + \mathrm{tr}(X\Omega)X,\quad \frac{\mathrm{d}\tau}{\mathrm{d}t} = (\tau - 1)\,\mathrm{tr}(X\Omega),\quad \Omega = -2L_+ = -2(\ell_0 I_2 + \ell_1\sigma^1), \tag{23}$$

a nonlinear channel with a purely non-Hermitian Hamiltonian $H = iL_+$ and no jump operators. In the Pauli basis,

$$\frac{\mathrm{d}r^a}{\mathrm{d}t} = G^{ab}r^b + C^a\tau,\ \ G = 2\ell_0 I_3 + \mathrm{tr}(X\Omega)I_3,\quad C = \ell_1\begin{pmatrix}2\\0\\0\end{pmatrix}. \tag{24}$$

The equations of motion are

$$\frac{\mathrm{d}x}{\mathrm{d}t} = 2\ell_0(1 - \tau)x + 2\ell_1(\tau - x^2), \tag{25}$$

$$\frac{\mathrm{d}y}{\mathrm{d}t} = 2\ell_0(1 - \tau)y - 2\ell_1 xy, \tag{26}$$

$$\frac{\mathrm{d}z}{\mathrm{d}t} = 2\ell_0(1 - \tau)z - 2\ell_1 xz. \tag{27}$$

In the $\tau = 1$ plane,

$$\frac{\mathrm{d}x}{\mathrm{d}t} = 2\ell_1(1 - x^2),\ \ \frac{\mathrm{d}y}{\mathrm{d}t} = -2\ell_1 xy,\quad \frac{\mathrm{d}z}{\mathrm{d}t} = -2\ell_1 xz. \tag{28}$$

Now there are two fixed points at $\boldsymbol{r}^{\mathrm{fp}}_\pm = (\pm 1, 0, 0)$. $\boldsymbol{r}^{\mathrm{fp}}_+$ is stable but $\boldsymbol{r}^{\mathrm{fp}}_-$ is not. Relative to the linear CPTP gate, the no-jump NINO gate adds a second fixed point at $\boldsymbol{r}^{\mathrm{fp}}_-$, but does not seem to offer any computational benefit. The velocity again

decreases linearly in $\delta = \tau - x \geqslant 0$ as the fixed point is approached.

2.3. One-jump NINO

Next we consider a NINO gate using the jump operator $B = B_0$ from the linear CPTP gate, but with $L_+ = 0$ and trace conserved nonlinearly. The equation of motion for the one-jump NINO channel is

$$\begin{aligned}\frac{\mathrm{d}X}{\mathrm{d}t} &= BXB^\dagger + \mathrm{tr}(X\Omega)X,\\ \frac{\mathrm{d}\tau}{\mathrm{d}t} &= (\tau - 1)\,\mathrm{tr}(X\Omega),\\ \Omega &= -B^\dagger B = 2m^2(\sigma^1 - I_2).\end{aligned} \tag{29}$$

$$\begin{aligned}\frac{\mathrm{d}r^a}{\mathrm{d}t} &= G^{ab}r^b + C^a\tau,\\ G &= m^2\begin{pmatrix}-2 & 0 & 0\\ 0 & 0 & 0\\ 0 & 0 & 0\end{pmatrix} + \mathrm{tr}(X\Omega)I_3,\\ C &= m^2\begin{pmatrix}2\\ 0\\ 0\end{pmatrix}.\end{aligned} \tag{30}$$

In the $\tau = 1$ plane,

$$\begin{aligned}\frac{\mathrm{d}x}{\mathrm{d}t} &= 2m^2(x-1)^2,\\ \frac{\mathrm{d}y}{\mathrm{d}t} &= 2m^2\,(x-1)y,\\ \frac{\mathrm{d}z}{\mathrm{d}t} &= 2m^2\,(x-1)z,\end{aligned} \tag{31}$$

which has a single fixed point at $\boldsymbol{r}^{\mathrm{fp}} = (1, 0, 0)$. To determine its stability, let $\delta = \tau - x \geqslant 0$ and rewrite (31) as

$$\frac{\mathrm{d}x}{\mathrm{d}t} = 2m^2\delta^2,\ \ \frac{\mathrm{d}y}{\mathrm{d}t} = -2m^2\delta\, y,\ \ \frac{\mathrm{d}z}{\mathrm{d}t} = -2m^2\delta\, z. \tag{32}$$

Inside the PSD cone, $\delta > 0$ and the motion is stable, but the critical slowing down is worse now because $\mathrm{d}x/\mathrm{d}t$ vanishes as δ^2 at the fixed point. Outside the PSD cone, however, the motion is unstable, and x increases without bound. The unstable region does not appear to be accessible dynamically when starting from the initial state $X = \frac{I_2}{2}$.

2.4. Pseudo-liner NINO

Next we consider a special subclass of NINO channels with $g = 1$ and $\Omega = \kappa I_2$ proportional to the identity. In this case the observable Ω vanishes except for a component in the I_2 direction. The equation of motion for the pseudo-liner NINO channel is

$$\begin{aligned}\frac{\mathrm{d}X}{\mathrm{d}t} &= \{L_+, X\} + \sum_\alpha \zeta_\alpha B_\alpha X B_\alpha^\dagger + g\kappa\tau X,\\ \frac{\mathrm{d}\tau}{\mathrm{d}t} &= (g\tau - 1)\kappa\tau,\ \ g = 1.\end{aligned} \tag{33}$$

Here the operators $L_+ \in \mathrm{Her}(\mathcal{H}, \mathbb{C})$ and $B_\alpha \in B(\mathcal{H}, \mathbb{C})$ are no longer independent; they are constrained to satisfy

$$\Omega = -2L_+ - \sum_\alpha \zeta_\alpha B_\alpha^\dagger B_\alpha = \kappa I_2,\ \ \kappa \in \mathbb{R}. \tag{34}$$

The condition $g = 1$ is required by trace conservation (applied to a $\tau = 1$ initial state). In this subclass the nonlinearity is effectively invisible, because

$$g\,\mathrm{tr}(X\Omega)X = g\kappa\tau X, \tag{35}$$

which acts linearly when restricted to the $\tau = 1$ plane. This implies a duality between pseudo-linear NINO channels and linear PTP channels. Assuming (33) and (34), the dual model is obtained by

$$L_+ \mapsto L_+ + \frac{\kappa}{2}I_2,\ \ g \mapsto 0. \tag{36}$$

We should think of (36) as being composed of two physically distinct steps. In the first step we shift $L_+ \mapsto L_+ + \frac{\kappa}{2}I_2$ while keeping $g = 1$, which [according to (9)] rescales $\Omega \mapsto 0$. It is important that $g = 1$ during this first step, as required by (11). However now that $\Omega = 0$, the trace can be conserved linearly, while violating condition (11). So in the second step we switch off the nonlinearity.

Consider the following example of a pseudo-linear NINO channel for a qubit: Combine the jump operator B_0 from the linear CPTP gate with $L_+ = \ell_1\sigma^1$, where $\ell_1 = m^2$. Then $\Omega = \kappa I_2$ with $\kappa = -2m^2$. In the Pauli basis

$$\frac{\mathrm{d}r^a}{\mathrm{d}t} = G^{ab}r^b + C^a\tau, \tag{37}$$

$$G = G_0 - 2m^2\tau I_3 = m^2\begin{pmatrix}-2-2\tau & 0 & 0\\ 0 & -2\tau & 0\\ 0 & 0 & -2\tau\end{pmatrix}, \tag{38}$$

$$C = C_{L_+} + C_0 = m^2\begin{pmatrix}4\\ 0\\ 0\end{pmatrix}. \tag{39}$$

In the $\tau = 1$ plane this leads to

$$\begin{aligned}\frac{\mathrm{d}x}{\mathrm{d}t} &= 4m^2(1-x),\ \ \frac{\mathrm{d}y}{\mathrm{d}t} = -2m^2y,\\ \frac{\mathrm{d}z}{\mathrm{d}t} &= -2m^2z,\end{aligned} \tag{40}$$

with same solution (22) as the linear CPTP gate. The nonlinearity in the pseudo-liner model is invisible in the Bloch ball picture but is apparent in the PSD cone, where it produces a fixed plane at $\tau = 1$. The fixed plane is lineary stable if $m \neq 0$. This form of nonlinearity does not appear to offer any computational advantage over the linear CPTP gate, as expected from the duality (36).

2.5. Three-jump NINO

Here we examine a three-jump NINO channel with a particularly striking fixed point structure due to the presence of fixed *lines* in the PSD cone. These fixed lines, when properly controlled, enable fast Bloch vector amplification without

deceleration. The equation of motion for the three-jump NINO channel is

$$\frac{\mathrm{d}X}{\mathrm{d}t} = \{L_+, X\} + \sum_\alpha \zeta_\alpha B_\alpha X B_\alpha^\dagger + g\,\mathrm{tr}(X\Omega)X,$$
$$\Omega = -2L_+ - \sum_\alpha \zeta_\alpha B_\alpha^\dagger B_\alpha. \tag{41}$$

Here the sum is over $\alpha = 1, 2, 3$, with Choi eigenvalue signs $\zeta_1 = 1, \zeta_2 = 1, \zeta_3 = -1$. The jump operators B_1, B_2, B_3 are given in table 1. In addition to these three jump operators we include a dissipative part $L_+ = \ell_\mu \sigma^\mu$, $\sigma^\mu = (I_2, \sigma^1, \sigma^2, \sigma^3)$, $\ell_\mu \in \mathbb{R}^4$. We do not include jump operator B_0 in this gate. $g \in \mathbb{R}$ is arbitrary. In the Pauli basis,

$$\frac{\mathrm{d}r^a}{\mathrm{d}t} = G^{ab} r^b + C^a \tau,$$
$$G = G_{L_+} + \sum_{\alpha=1}^3 \zeta_\alpha G_\alpha + g\,\mathrm{tr}(X\Omega) I_3,$$
$$C = C_{L_+} + \sum_{\alpha=1}^3 \zeta_\alpha C_\alpha. \tag{42}$$

Then

$$G = \mathrm{tr}(L_+) I_3 + m_1^2 \begin{pmatrix} 0 & 2 & 0 \\ 2 & 0 & 0 \\ 0 & 0 & -2 \end{pmatrix} + m_2^2 \begin{pmatrix} 0 & 0 & 0 \\ 0 & 0 & 0 \\ 0 & 0 & 2 \end{pmatrix} - m_3^2 \begin{pmatrix} -1 & 0 & 0 \\ 0 & -1 & 0 \\ 0 & 0 & 1 \end{pmatrix} + g\,\mathrm{tr}(X\Omega) I_3, \tag{43}$$

$$C = C_{L_+} + C_2 = \begin{pmatrix} 2\ell_1 \\ 2\ell_2 \\ 2\ell_3 \end{pmatrix} + m_2^2 \begin{pmatrix} 0 \\ 0 \\ 2 \end{pmatrix}. \tag{44}$$

Next we set the jump operator strengths to be

$$m_1 = \sqrt{M/2}\,,\ \ m_2 = \sqrt{M/2}\,,\ \ m_3 = \sqrt{M - \tfrac{\Gamma}{2}}\,, \tag{45}$$

where

$$M \geqslant \frac{\Gamma}{2} \geqslant 0. \tag{46}$$

With these settings

$$G = \mathrm{tr}(L_+) I_3 + \begin{pmatrix} 0 & M & 0 \\ M & 0 & 0 \\ 0 & 0 & 0 \end{pmatrix} + \begin{pmatrix} M - \frac{\Gamma}{2} & 0 & 0 \\ 0 & M - \frac{\Gamma}{2} & 0 \\ 0 & 0 & \frac{\Gamma}{2} - M \end{pmatrix} + g\,\mathrm{tr}(X\Omega) I_3, \tag{47}$$

$$C = \begin{pmatrix} 2\ell_1 \\ 2\ell_2 \\ 2\ell_3 \end{pmatrix} + \begin{pmatrix} 0 \\ 0 \\ M \end{pmatrix}, \tag{48}$$

$$\sum_{\alpha=1}^3 \zeta_\alpha B_\alpha^\dagger B_\alpha = 2m_1^2 I_2 + 2m_2^2 (I_2 + \sigma^3) - m_3^2 I_2 = \left(M + \tfrac{\Gamma}{2}\right) I_2 + M\sigma^3, \tag{49}$$

$$\Omega = -2L_+ - \left(M + \tfrac{\Gamma}{2}\right) I_2 - M\sigma^3. \tag{50}$$

Next we choose $L_+ = -(M/2)\sigma^3$ to tune the σ^3 component of Ω to zero, leading to a pseudo-linear channel:

$$\Omega = -\left(M + \tfrac{\Gamma}{2}\right) I_2,\ \ \mathrm{tr}(X\Omega) = -\left(M + \tfrac{\Gamma}{2}\right)\tau. \tag{51}$$

According to (12), however, when $g = 1$ the resulting channel satisfies

$$\left(\frac{\mathrm{d}X}{\mathrm{d}t}\right)_{\frac{I_2}{2}} = 0 \tag{52}$$

and is therefore unital. This would seem to preclude its use for Bloch vector amplification, but this conclusion does not apply if the fixed point is unstable. In the pseudo-linear case (51) we have

$$G = \begin{pmatrix} M - \frac{\Gamma}{2} & M & 0 \\ M & M - \frac{\Gamma}{2} & 0 \\ 0 & 0 & \frac{\Gamma}{2} - M \end{pmatrix} - \tau\left(M + \tfrac{\Gamma}{2}\right) I_3,\ \ C = 0. \tag{53}$$

Finally, upon restriction to the $\tau = 1$ plane and $g = 1$ we obtain the following qubit equation of motion in the three-jump NINO model:

$$\frac{\mathrm{d}r^a}{\mathrm{d}t} = G^{ab} r^b,\ \ G = \begin{pmatrix} -\Gamma & M & 0 \\ M & -\Gamma & 0 \\ 0 & 0 & -2M \end{pmatrix},$$
$$M, \Gamma \in \mathbb{R},\ \ M \geqslant \frac{\Gamma}{2} \geqslant 0. \tag{54}$$

Let us examine the equations of motion for the model (54), which is similar to a model investigated in [35] but now without torsion:

$$\frac{\mathrm{d}x}{\mathrm{d}t} = -\Gamma x + My,\ \ \frac{\mathrm{d}y}{\mathrm{d}t} = -\Gamma y + Mx,$$
$$\frac{\mathrm{d}z}{\mathrm{d}t} = -2Mz. \tag{55}$$

If $M \neq \Gamma$ the channel has a single fixed point $\boldsymbol{r}_0^{\mathrm{fp}} = (0, 0, 0)$ at the center of the Bloch ball. To examine its stability, switch to rotated coordinates

$$\xi_\pm := \frac{y \pm x}{2}. \tag{56}$$

Then

$$\frac{\mathrm{d}\xi_+}{\mathrm{d}t} = (M - \Gamma)\,\xi_+,\ \ \frac{\mathrm{d}\xi_-}{\mathrm{d}t} = -(M + \Gamma)\,\xi_-. \tag{57}$$

Note that if $M = \Gamma$, the entire ξ_+ axis (the line $y = x$, $z = 0$) is a fixed *line* of the map. If $M \neq \Gamma$, there are no fixed lines and the ξ_+ axis flows toward or away from $\boldsymbol{r}_0^{\mathrm{fp}}$. The ξ_+ direction is stable for $M < \Gamma$ but is unstable for $M > \Gamma$. Therefore when $M > \Gamma$ the

fixed point $\boldsymbol{r}_0^{\rm fp}$ becomes unstable. The instability of the fixed point at $X = \frac{I_2}{2}$ allows this unital channel to be used for Bloch vector amplification. The solution giving the desired amplification gate for $M > \Gamma$ is

$$\begin{aligned} x(t) &= y(t) = \mathrm{e}^{(M-\Gamma)t} - 1, \\ x(t_{\rm gate}) &= y(t_{\rm gate}) = \frac{\tau}{\sqrt{2}}, \\ t_{\rm gate} &= \frac{\log\left(1 + \frac{\tau}{\sqrt{2}}\right)}{M - \Gamma}, \ z = 0. \end{aligned} \tag{58}$$

Note that the ξ_- direction is always stable in this model. This is a great improvement over the linear CPTP gate because it does not decelerate.

An amplification gate based on the three-jump NINO model (54) requires a small modification due to the instability at the starting point $X = \frac{I_2}{2}$. The simplest modification would be to initialize the qubit slightly away from $\boldsymbol{r} = (0,\ 0,\ 0)$ before switching on the nonlinearity. This can be achieved by applying the linear CPTP amplification gate for a short duration to pre-amplify the state to $\boldsymbol{r} = (x,\ 0,\ 0)$ with small positive x. In the rotated frame the pre-amplified state is

$$\xi_+ = \frac{x}{2}, \ \xi_- = -\frac{x}{2}, \ 0 < x \ll 1. \tag{59}$$

Applying the three-jump NINO channel then successfully amplifies the qubit state.

2.6. Linear non-CP

The final model we consider is motivated by the three-jump gate (58), which supports fast Bloch vector amplification without deceleration. As explained above, the NINO model (4) is invariant under a shift (8) of the dissipative part L_+ of the non-jump component of the linear infinitesimal generator.[2] Furthermore, in the special case of a pseudo-linear NINO channel (section 2.4), where the observable Ω is proportional to the identity, the invariance leads to the duality (36) between pseudo-linear NINO channels with $g = 1$ and strictly linear channels with $g = 0$. Here we use this duality to construct a linear non-CP channel and gate equivalent to those of section 2.5, specifically to the pseudo-linear model (51). The equivalent linear non-CP model, an instance of (16), is

$$\begin{aligned} \frac{\mathrm{d}X}{\mathrm{d}t} &= \{L_+, X\} + \sum_\alpha \zeta_\alpha B_\alpha X B_\alpha^\dagger, \\ \frac{\mathrm{d}\tau}{\mathrm{d}t} &= 0, \ L_+ = -\frac{1}{2}\sum_\alpha \zeta_\alpha B_\alpha^\dagger B_\alpha, \ g = 0. \end{aligned} \tag{60}$$

Here the sum is over $\alpha = 1,\ 2,\ 3$, with signs $\zeta_1 = 1$, $\zeta_2 = 1$, $\zeta_3 = -1$, indicating a non-CP channel [37–40]. The jump operators B_1, B_2, B_3 are given in table 1 and are the same as in section 2.5. In addition to these jump operators we include the L_+ specified in (60). Then

$$\frac{\mathrm{d}r^a}{\mathrm{d}t} = G^{ab} r^b + C^a \tau, \tag{61}$$

where, after using (45),

$$\begin{aligned} G &= \mathrm{tr}(L_+) I_3 + \begin{pmatrix} M - \frac{\Gamma}{2} & M & 0 \\ M & M - \frac{\Gamma}{2} & 0 \\ 0 & 0 & \frac{\Gamma}{2} - M \end{pmatrix}, \\ C &= \begin{pmatrix} 2\ell_1 \\ 2\ell_2 \\ 2\ell_3 \end{pmatrix} + \begin{pmatrix} 0 \\ 0 \\ M \end{pmatrix}, \end{aligned} \tag{62}$$

where

$$L_+ = -\frac{\left(M + \frac{\Gamma}{2}\right) I_2 + M\sigma^3}{2}, \ \mathrm{tr}(L_+) = -\left(M + \tfrac{\Gamma}{2}\right). \tag{63}$$

Then $\ell_1 = \ell_2 = 0$ and $\ell_3 = -\frac{M}{2}$, leading to

$$\begin{aligned} \frac{\mathrm{d}r^a}{\mathrm{d}t} &= G^{ab} r^b, \ G = \begin{pmatrix} -\Gamma & M & 0 \\ M & -\Gamma & 0 \\ 0 & 0 & -2M \end{pmatrix}, \\ C &= 0, \ M, \Gamma \in \mathbb{R}, \ M \geqslant \frac{\Gamma}{2} \geqslant 0, \end{aligned} \tag{64}$$

as in (54). This supports the fast amplification gate (58) without requiring nonlinearity.

3. Conclusions

In this paper we have investigated several designs for Bloch vector amplification gates based on linear and nonlinear PTP channels, which offer benefits relative to linear CPTP channels for this application. We do not consider microscopic models for these channels, but instead think of them as effective Markovian models for engineered strongly correlated quantum materials coupled to their environment. Thus, the models only satisfy the minimal properties of positivity and trace preservation. Our results indicate that, while non-CP dynamics is essential for fast Bloch vector amplification, NINO-type nonlinearity offers no additional computational benefit. This is because the instability underlying the gate (58) does not result from nonlinearity but instead from a competition between gain M and dissipation Γ.

Although we have only considered channels from class (i) and (ii), this was sufficient to achieve a significant improvement over the linear CPTP gate. In the future it would be interesting to consider amplification gates from classes (iii) and (iv) as well. Such gates might provide additional design benefits, such as robustness to noise. Finally, we note that the linear non-CP gate proposed here should be practical to realize, as it only requires linear operations on an open system with initial system-environment entanglement. It is well known that time-reversal transformations can be simulated on

[2] Recall that iL_+ is an anti-Hermitian but otherwise arbitrary qubit Hamiltonian. The Hermitian part of the Hamiltonian vanishes here because amplification is nonunitary.

a quantum computer by implementing complex conjugation or reversing the sign of a simulated Hamiltonian [45, 46]. Similarly, fast Bloch vector amplification gates can be used to simulate a reversal of the thermodynamic arrow of time [47–50] for a qubit, and would constitute a striking demonstration physical non-CP dynamics.

Acknowledgments

This work was partly supported by the NSF under Grant No. DGE-2152159.

ORCID iDs

Michael R Geller https://orcid.org/0000-0003-3226-1101

References

[1] Mielnik B 1980 Mobility of nonlinear systems *J. Math. Phys.* **21** 44
[2] Abrams D S and Lloyd S 1998 Nonlinear quantum mechanics implies polynomial-time solution for NP-Complete and $\#P$ problems *Phys. Rev. Lett.* **81** 3992
[3] Bechmann-Pasquinucci H, Huttner B and Gisin N 1998 Nonlinear quantum state transformation of spin-1/2 *Phys. Lett.* A **242** 198
[4] Czachor M 1998 Notes on nonlinear quantum algorithms *Acta Phys. Slov.* **48** 157
[5] Czachor M Local modification of the Abrams–Lloyd nonlinear algorithm arXiv:quant-ph/9803019
[6] Terno D R 1999 Nonlinear operations in quantum-information theory *Phys. Rev.* A **59** 3320
[7] Bacon D 2004 Quantum computational complexity in the presence of closed timelike curves *Phys. Rev.* A **70** 032309
[8] Aaronson S NP-complete problems and physical reality arXiv: quant-ph/0502072
[9] Brun T A, Harrington J and Wilde M M 2009 Localized closed timelike curves can perfectly distinguish quantum states *Phys. Rev. Lett.* **102** 210402
[10] Bennett C H, Leung D, Smith G and Smolin J A 2009 Can closed timelike curves or nonlinear quantum mechanics improve quantum state discrimination or help solve hard problems? *Phys. Rev. Lett.* **103** 170502
[11] Kahou M E and Feder D L 2013 Quantum search with interacting Bose–Einstein condensates *Phys. Rev.* A **88** 032310
[12] Meyer D A and Wong T G 2013 Nonlinear quantum search using the Gross–Pitaevskii equation *New J. Phys.* **15** 063014
[13] Meyer D A and Wong T G 2014 Quantum search with general nonlinearities *Phys. Rev.* A **89** 012312
[14] Childs A M and Young J 2016 Optimal state discrimination and unstructured search in nonlinear quantum mechanics *Phys. Rev.* A **93** 022314
[15] Di Molfetta G and Herzog B Searching via nonlinear quantum walk on the 2D-grid arXiv:2009.07800
[16] Deffner S 2022 Nonlinear speed-ups in ultracold quantum gases *Europhys. Lett.* **140** 48001
[17] Xu J, Schmiedmayer S and Sanders B C 2022 Nonlinear quantum gates for a Bose–Einstein condensate *Phys. Rev. Res.* **4** 023071
[18] Gisin N 1981 A simple nonlinear dissipative quantum evolution equation *J. Phys. A: Math. Gen.* **14** 2259
[19] Alicki R and Messer J 1983 Nonlinear quantum dynamical semigroups for many-body open systems *J. Stat. Phys.* **32** 299
[20] Breuer H-P and Petruccione F 2002 *The Theory of Open Quantum Systems* (Oxford University Press)
[21] Drossel B What condensed matter physics and statistical physics teach us about the limits of unitary time evolution arXiv:1908.10145
[22] Gisin N and Cibils M B 1992 Quantum diffusions, quantum dissipation and spin relaxation *J. Phys.* A **25** 5165
[23] Brody D C and Graefe E-M 2012 Mixed-state evolution in the presence of gain and loss *Phys. Rev. Lett.* **109** 230405
[24] Zloshchastiev K G and Sergi A 2014 Comparison and unification of non-Hermitian and Lindblad approaches with applications to open quantum optical systems *J. Mod. Opt.* **61** 1298
[25] Dominy J M and Lidar D A 2016 Beyond complete positivity *Quantum Inf. Process.* **15** 1349
[26] Kowalski K and Rembieliński J 2019 Integrable nonlinear evolution of the qubit *Ann. Phys.* **411** 167955
[27] Kowalski K 2020 Linear and integrable nonlinear evolution of the qutrit *Quant. Inf. Proc.* **19** 145
[28] Fonseca Romero K M, Talkner P and Hänggi P 2004 Is the dynamics of open quantum systems always linear? *Phys. Rev.* A **69** 052109
[29] Fernengel B and Drossel B 2020 Bifurcations and chaos in nonlinear Lindblad equations *J. Phys. A: Math. Theor.* **53** 385701
[30] Rembieliński J and Caban P 2020 Nonlinear extension of the Quantum dynamical semigroup *Quantum* **5** 420
[31] Buks E and Schwartz D 2021 Stability of the Grabert master equation *Phys. Rev.* A **103** 052217
[32] Kłobus W, Kurzyński P, Kuś M, Laskowski W, Przybycień R and Życzkowski K Transition from order to chaos in reduced quantum dynamics arXiv:2111.13477
[33] Gorini V, Kossakowski A and Sudarshan E C G 1976 Completely positive dynamical semigroups of N-level systems *J. Math. Phys.* **17** 821
[34] Lindblad G 1976 On the generators of quantum dynamical semigroups *Comm. Math. Phys.* **48** 119
[35] Geller M R 2023 Fast quantum state discrimination with nonlinear PTP channels *Adv. Quantum Technol.* **6** 2200156
[36] Rembieliński J and Caban P 2020 Nonlinear evolution and signaling *Phys. Rev. Res.* **2** 012027
[37] Pechukas P 1994 Reduced dynamics need not be completely positive *Phys. Rev. Lett.* **73** 1060
[38] Shaji A and Sudarshan E C G 2005 Who's afraid of not completely positive maps? *Phys. Lett.* A **341** 48
[39] Carteret H A, Terno D R and Życzkowski K 2008 Dynamics beyond completely positive maps: some properties and applications *Phys. Rev.* A **77** 042113
[40] Dominy J M, Shabani A and Lidar D A 2016 A general framework for complete positivity *Quantum Inf. Process.* **15** 465
[41] Peres A 1996 Separability criterion for density matrices *Phys. Rev. Lett.* **77** 1413
[42] Gregoratti M and Werner R F 2004 On quantum error correction by classical feedback in discrete time *J. Math. Phys.* **45** 2600
[43] Hayden P and King C 2005 Correcting quantum channels by measuring the environment *Quant. Inf. Comp.* **5** 156
[44] Winter A On environment-assisted capacities of quantum channels arXiv:quant-ph/0507045
[45] Zhang X, Shen Y, Zhang J, Casanova J, Lamata L, Solano E, Yung M-H, Zhang J-N and Kim K 2015 Time reversal and charge conjugation in an embedding quantum simulator *Nat. Comm.* **6** 7917

[46] Lesovik G B, Sadovskyy I A, Suslov M V, Lebedev A V and Vinokur V M 2019 Arrow of time and its reversal on the IBM quantum computer *Sci. Rep.* **9** 4396
[47] Lebowitz J L 1993 Macroscopic laws, microscopic dynamics, time's arrow and Boltzmann's entropy *Physica* A **194** 1
[48] Jennings D and Rudolph T 2010 Entanglement and the thermodynamic arrow of time *Phys. Rev.* E **81** 061130
[49] Campisi M and Hänggi P 2011 Fluctuation, dissipation and the arrow of time *Entropy* **13** 2024
[50] Mastroserio I, Gherardini S, Lovecchio C, Calarco T, Montangero S, Cataliotti F S and Caruso F 2022 Experimental realization of optimal time-reversal on an atom chip for quantum undo operations *Adv. Quantum Technol.* **5** 2200057